Using a new 4D Digital Holographic PIV/PTV (4D-DHPIV/PTV) Methodology to Measure Wall-bounded Shear Flows

Bihai Sun[1]*, Asif Ahmed[1], Callum Atkinson[1] and Julio Soria[1]

[1]Laboratory for Turbulence Research in Aerospace & Combustion (LTRAC)

Department of Mechanical and Aerospace Engineering

Monash University (Clayton Campus)

Melbourne, VIC 3800 AUSTRALIA

*bihai.sun@monash.edu

Abstract

This paper presents an advanced inline 4-dimensional (3D-3C) digital holographic PIV/PTV technique, which not only contains conventional direct reconstruction approach, but also incorporates advanced digital filtering to remove the virtual image effect, 3-dimensional volume deconvolution to reduce the depth-of-focus problem and the virtual image, an efficient one-pass 3-dimensional clustering algorithm coupled with a new predictive inverse reconstruction approach based on previous work in this area, to increase the particle reconstruction dynamic range and 3-dimensional reconstruction domain. The method is then verified by measuring the velocity profile in a laminar micro-channel flow and the result is compared to analytical solution.

1   Introduction

Wall-bounded turbulent flows are inherently three-dimensional (3D) in nature containing a broad range of flow structures, turbulent length scales and dynamic range. All these features necessitate a measurement technique which is able to quantify and investigate these flows by measuring the instantaneous three-component three- dimensional (3C-3D) velocity vector with high spatial and temporal resolution. Over the last few decades, a number of techniques such as Tomographic PIV (TPIV), synthetic aperture PIV (SAPIV), light-field PIV (LFPIV) etc. have shown great promises to yield three-dimensional information of turbulent flow field, however, these techniques are still inadequate for the investigation of wall-bounded turbulent flows due to their limited spatial and temporal resolution or their limited access to the measurement area.

3D photogrammetry Malik et al. (1993b,a); Sato et al. (1994) coupled with cross-correlation PIV analysis also known as Tomographic PIV (TPIV) Ciofalo et al. (2003); Elsinga et al. (2006); Atkinson and Soria (2009) is one of the techniques which can provide 3C-3D velocity fields of unsteady and/or turbulent flows, however, it suffers from severe limitations in spatial resolution Atkinson et al. (2011).

A recently developed alternative, instead of recording the three-dimensional position of tracer particles through the multiple view geometry of TPIV, uses light-field imaging to record the particle light-field image via a single plenoptic camera Adelson and Wang (1992) which consists of a closely

encapsulated micro-lens array (MLA) and a CCD/CMOS sensor. When coupled with cross-correlation PIV analysis it yields 3C-3D velocimetry technique, referred to as light-field PIV (LFPIV) Fahringer et al. (2015); Shi et al. (2017, 2018). LFPIV has compact hardware setup similar as 2D-PIV and eliminates the cumbersome camera spatial calibration process, which is essential and a major source of error in TPIV. Although LFPIV is capable of measuring full volumetric 3C-3D velocity fields, the pixel-to-microlens ratio (PMR) is the key factor that limits the performance of LFPIV.

In the early days film-based holographic PIV (HPIV) showed great promise [Barnhart et al. (1994); Hussain et al. (1993); Lozano et al. (1999); Ellenrieder et al. (2001)], however, the physical or chemical processing of recording materials made its implementation complicated and limited its success in developing into a standard laboratory tool. More recently, digital holographic recording and reconstruction Coëtmellec et al. (2001); Murata and Yasuda (2000); Pan and Meng (2003); von Ellenrieder and Soria (2003); Lobera et al. (2004); Palero et al. (2007) coupled with cross-correlation PIV analysis (DHPIV) has shown promise as a 3C-3D velocity field measurement tool, but it too has its shortcoming, such as extended depth-of-focus (DOF) problem where elongation of the tracer particles in depth direction causes poor longitudinal resolution, the virtual image effect, limitation on seeding density which in turn limits the spatial resolution of velocity field, human interventions in different stages of postprocessing, etc.

This present study involves a novel in-line 4D-DHPIV/PTV methodology which in addition to including the standard digital hologram reconstruction, incorporates advanced automatic digital filtering to reduce human interventions, 3-dimensional volume deconvolution to reduce the depth-of-focus problem and the virtual image effect, an efficient one-pass 3-dimensional clustering algorithm coupled with a new predictive inverse reconstruction approach based on previous work in this area, to increase the particle reconstruction dynamic range and 3-dimensional reconstruction domain. The methodology will be experimentally tested against the theoretical velocity profile in a laminar micro-channel flow.

2 Digital Holographic PIV - Direct Reconstruction

By digital hologram recording and reconstruction, DHPIV can produce a three-dimensional particle intensity field from a single image produced by one single camera, without the complex optical arrangement and calibration process, which is essential in some 3D fluid flow measurement methods like TPIV. Thus, two sequentially recorded 3D intensity fields of all particles can subsequently be analysed using 3D cross-correlation analysis as is done in TPIV or a hybrid cross-correlation PIV - PTV approach can also be used Soria et al. (2014) to enhance the spatial resolution to the particle size level.

This paper primarily concerns with the in-line configuration of holography, but the same method is applicable to other configurations with some modification. In the in-line configuration, a collimated planer laser beam with sufficient diameter to cover the measurement volume is used to illuminate micron or sub-micro sized tracer particles. The unobstructed laser beam acts as the reference beam, which interference with the scattered light from particles to produce a fringe pattern, and the intensity of the pattern is recorded by camera sensor to form a digital hologram.

The digital reconstruction process models how the hologram is reconstructed optically. The hologram intensity distribution recorded on the electronic sensor, which is identified by the Cartesian coordinate system $(x, y, z = 0)$, is multiplied by the reference (or its conjugate) wave and the resulting wave $IH(x;y;0)$ is numerically propagated to the virtual (or real) image plane. The complex amplitude distribution $U(x0;y0; z)$ in any plane, which is a distance z normal from the

hologram position, i.e. from the electronic sensor plane, can be calculated from IH(x;y;0) using the Rayleigh–Sommerfeld diffraction formula Goodman (1996),

$$U(x_0, y_0; z) = \frac{1}{i\lambda} \int_\Sigma \frac{I_H(x,y,0)(\exp(ikr_{01}))}{r_{01}} \cos(\vec{n}, \overrightarrow{r_{01}}) \, dxdy \tag{1}$$

In this equation, λ and $k = \frac{2\pi}{\lambda}$ is the wavelength and wavenumber respectively of the illumination used during the recording of the digital hologram. $r_{01} = \sqrt{(x_0 - x)^2 + (y_0 - y)^2 + z}$ in the equation represents the distance from a point on the hologram (x,y,0) to any points in the reconstruction image (x0,y0,z) which is located distance z away from the hologram. The obliquity factor, $\cos(\vec{n}, \overrightarrow{r_{01}})$, can be approximated by 1 in most cases, as the distance between the reconstruction image and hologram is typically bigger than the camera array size. Thus, the above equation can be written into a convolution form,

$$U(x_0, y_0; z) = I_H(x, y, 0) \otimes h(x_0, y_0, z; x, y) \tag{2}$$

Where h is wave propagation kernel and $\otimes$ represents the convolution operator. The above equation is easier calculated in the Fourier space, as the convolution can be calculated by multiplication in Fourier space, thus the reconstruction image can be numerically propagated as

$$U(x_0, y_0; z) = \mathcal{F}^{-1}\left(\mathcal{F}\big(I_H(x, y, 0)\big) \times H\big(f_x, f_y, z\big)\right) \tag{3}$$

Here, $\mathcal{F}()$ represents the Fourier transform, and $H\big(f_x, f_y, z\big)$, the propagation kernel in Fourier space can be calculated from:

$$H\big(f_x, f_y, z\big) = e^{\left(\frac{j2\pi z}{\lambda}\sqrt{1 - \lambda f_x^2 - \lambda f_y^2}\right)} \tag{4}$$

Using direct reconstruction, although the particles can be reconstructed from hologram, there is big uncertainty in the z location of the particle, as the particle is greatly elongated. A sample reconstruction of a particle is shown in the following figure:
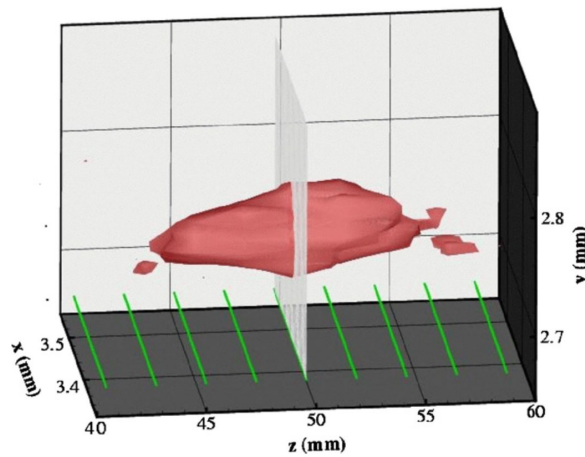

Figure 1: Digital hologram reconstruction of a 90 μm diameter particle recorded using in-line digital holography. The central plane at z = 49.7 mm is shown as a grey sheet and the green lines correspond to the locations of the other reconstruction planes von Ellenrieder and Soria (2003).

The above figure shows that the 90 μm diameter particle appears to have a major diameter of 15.2mm, which is highly unphysical and adversely affect the accuracy of the centroid of the particle. One way to solve this depth-of-field problem is utilising more advanced reconstruction method, as discussed below.

3   Digital Holographic PIV - Advanced Reconstruction Approach

A number of steps are used in the advanced reconstruction approach to improve the accuracy of the particle location in the volume as a basis of PIV analysis. The first additional process is to apply a three-dimensional (3D) deconvolution step introduced by Latychevskaia et al. (2010) using a point-spread function (PSF) to the direct hologram reconstruction, which reconstruct the true 3D amplitude distribution of objects. The deconvolution not only greatly reduces the depth of focus, but also removes the virtual image, as they are both present in the point spread function. The point spread function of the system can be determined both experimentally and analytically. Experimentally, the hologram produced by a single particle can be propagated to each z location in direct reconstruction, then use that as point spread function. Otherwise, the particle can be modelled as an aperture in x-y plane, and the image of the aperture is propagated to both positive and negative positions to yield a point spread function. Once the point spread function is obtained, the deconvolved volume can be calculated by:

$$U_{real}(x_0, y_0; z) = \mathcal{F}^{-1}\left(\frac{\mathcal{F}(U(x_0,y_0;z))}{\mathcal{F}(U_{psf}(x,y,z))}\right) \tag{5}$$

where $U_{Real}(x_0, y_0; z)$ is the 3D-deconvolved complex amplitude distribution and $U_{PSF}(x, y; z)$ is the 3D point-spread function. In order to avoid dividing by zero, a small number can be added to the point spread function. Also, a filter in Fourier space can be applied after division to remove high frequency noise.

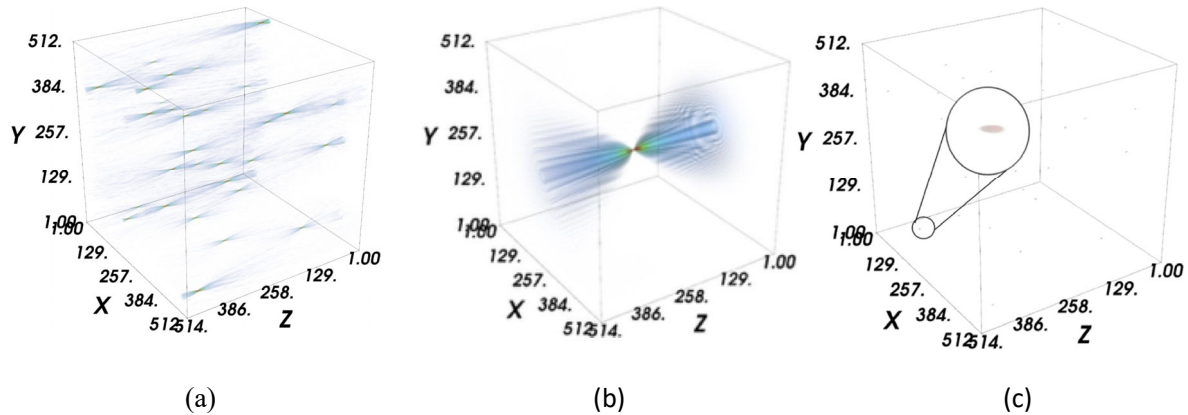(a)   (b)   (c)

Figure 2: (a) Typical 3D direct hologram reconstruction of particles, (b) point-spread function, (c) 3D-deconvolved reconstruction of particles, showing vast improvement in particle position.

The deconvolved volume then undergoes a segmentation process via an efficient one-pass 3-dimensional Hoshen Kopelman (HK) clustering algorithm Hoshen and Kopelman (1976). An optimal threshold can be selected by analyzing the number of clusters found for each threshold, then the rough positions of the particles are extracted from the deconvolved volume by clustering. The rough particle positions from this step then undergoes an inverse reconstruction and particle removal process, as by Soulez et al. (2007) to further improve the location of the particles, as well as detect

particles which are either in the shadow of particles, are weak scatters, or are in fact outside the projected area of the sensor.

Once a sequential pair of 3D holograms has been reconstructed, these can be analyzed using 3D cross- correlation analysis or a hybrid cross-correlation PIV - PTV at the particle spatial resolution level Soria et al. (2014) to reveal the 3C-3D fluid velocity field. Furthermore, since a time series of digital holograms is avail- able in this 4D-DHPIV/PTV methodology, then once 3-4 3C-3D velocity fields are available, quite accurate predictive positions of the particle locations can be used to accelerate the inverse hologram reconstruction step

4   Application of Digital Holographic PIV to Micro-Channel Flow

In order to test the DHPIV in real life situation, the method is used to measure a laminar flow in a micro channel. The experiment set up is as the following figure.
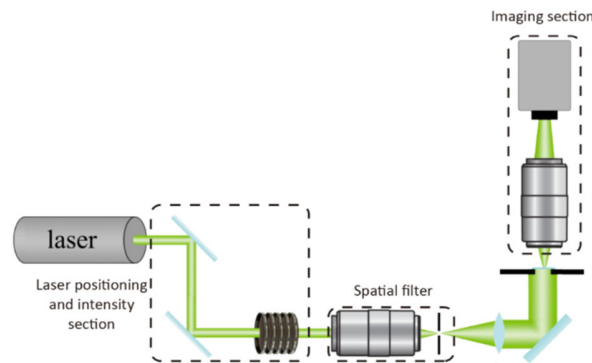

Figure 3: The experimental set up to measure the micro-channel flow

The illumination source used was a continuous solid-state laser with wavelength 532nm and power 500mW. After neutral density filters, the laser beam was spatially filtered to produce a clean Gaussian profile. The clean beam was then collimated to achieve plane reference wave which illuminated a single channel of a multi-channel glass microfluidic chip (Micronit flow cell). The channel used for this study was 50μm high, 1.5mm wide and 40mm long. Polystyrene microsphere (Polysciences Inc.) of nominal diameter of 1 μm was used to seed the flow and an off-chip syringe pump (KD Scientific) was employed to provide the continuous laminar flow in the microchannel. The lens used was an infinitely-corrected microscope lens with numerical aperture of 0.2, working at magnification of 9.07x. The camera (ILA.PIV.sCMOS) sensor resolution used for the recording of holograms was 2560 x 2160 with physical pixel size of 6.5μm, the effective pixel size after magnified by the microscope lens is 0.71μm. The holograms were taken at a frame rate of 15 fps.

As the width of the microchannel is 30 times of its height, the flow in the micro-channel can be modelled as a planar channel flow, thus the velocity profile across height direction can be analytically calculated by plane Poiseuille flow solution, which is given by J. Anderson Jr (2010):

$$u(y) = \frac{G}{2\mu} \times y \times (h - y) \tag{6}$$

Where G is the pressure gradient in the channel and can be calculated from the volume flow rate per unit width in the channel.

$$Q = \frac{Gh^3}{12\mu} \tag{7}$$

Thus, the velocity profile of streamwise velocity in channel height direction can be plotted and compared to analytical solution, as below:
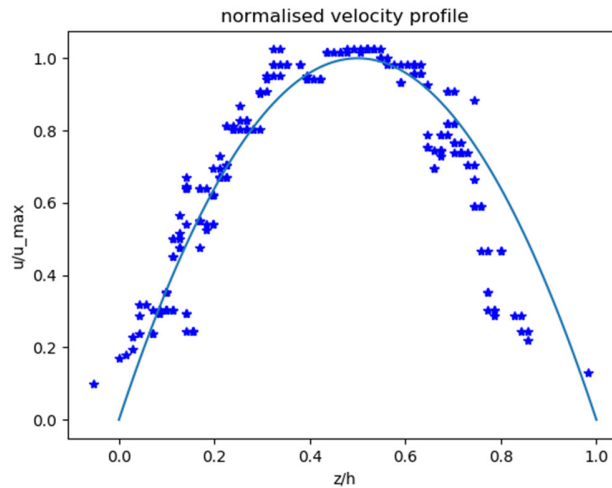

Figure 4: The streamwise velocity profile across the height of the channel. Dots: measurement from DHPIV. Line: analytical solution

The average difference between the analytical and measured velocity across the channel height is -2.9% of the maximum velocity in the channel, which means on average the measured flow is slower than the analytical solution. The RMS error between the measured and analytical solution is, however, over 10 % of maximum velocity in the channel, which suggest the reconstruction techniques still need improvement. Also, from the above figure, the difference between the measured and real velocity increases as z increases, suggesting the particles are not completely removed in the particle removal process, thus the residual from improperly deleted particles in the front interfered with the inverse process of the particles further away and produced poor reconstruction.

5 Conclusion

This paper describes the details of direct digital hologram reconstruction and discusses some of its shortcomings. An in-line 4-dimensional (i.e. time-resolved 3C-3D) digital holographic PIV/PTV (4D-DHPIV/PTV) method is presented which overcomes these shortcomings. This 4D-DHPIV/PTV method, in addition to including the standard digital hologram reconstruction, incorporates 3-dimensional volume deconvolution to reduce the depth-of-focus problem and the virtual image, an efficient one-pass 3-dimensional HK clustering algorithm coupled with a novel predictive inverse reconstruction approach and particle deletion, based on previous work in this area.

The DHPIV technique is also verified in experiment by measuring laminar channel flow. The experiment reveals this velocity profile measured has a 3% of maximum velocity bias error and 10% of maximum velocity RMS error compared to the analytical solution.

Acknowledgements

References

Adelson EH and Wang JYA (1992) Single Lens Stereo with a Plenoptic Camera. *IEEE Transactions on Pattern Analysis and Machine Intelligence* 14:99–106

Anderson, J (2010) *Fundamentals of Aerodynamics*. McGraw-Hill. 5th ed.

Atkinson C, Coudert S, Foucaut JM, Stanislas M, and Soria J (2011) The accuracy of tomographic particle image velocimetry for measurements of a turbulent boundary layer. *Experiments in fluids* 50:1031–1056

Atkinson C and Soria J (2009) An efficient simultaneous reconstruction technique for tomographic particle image velocimetry. *Experiments in Fluids* 47:553–568

Barnhart D, Adrian R, and Papen G (1994) Phase-conjugate holographic system for high resolution particle image velocimetry. *Applied Optics* 33:7159–7170

Ciofalo M, Signorin M, and Simiano M (2003) Tomographic particle image velocimetry and thermography in Rayleigh-B6nardconvectionusingsuspendedthermochromic liquid crystals and digital image processing. *Experiments in Fluids* 34:156–172

Coëtmellec S, Buraga-Lefebvre C, Lebrun D, and Ozkul C (2001) Application of in-line digital holography to multiple plane velocimetry. *Measurement Science and Technology* 12:1392–1397

Ellenrieder Kv, Kostas J, and Soria J (2001) Measurements of a wall-bounded turbulent, separated flow using HPIV. *Journal of Turbulence* 2:1–15

Elsinga GE, Scarano F, Wieneke B, and Van Oudheusden B (2006) Tomographic particle image velocimetry. *Experiments in Fluids* 41:933–947

Fahringer TW, Lynch KP, and Thurow BS (2015) Volumetric particle image velocimetry with a single plenoptic camera. *Measurement Science and Technology* 26:115201

Goodman JW (1996) *Introduction to Fourier Optics*. McGraw-Hill. second edition edition

Hoshen J and Kopelman R (1976) Percolation and cluster distribution. I. Cluster multiple labeling technique and critical concentration algorithm. *Physical Review B (Solid State)* 14:3438–3445

Hussain F, Liu DD, Simmonds S, and Meng H (1993) Hpiv prospects and limitations holographic particle image velocimetry. *FED* 148:1–11

Lobera J, Andrés N, and Arroyo MP (2004) Digital speckle pattern interferometry as a holographic velocimetry technique. *Measurement Science and Technology* 15:718–724

Lozano A, Kostas J, and Soria J (1999) Use of holography in particle image velocimetry measurements of a swirling flow. *Experiments in Fluids* 27:251—261

Malik N, Dracos T, and Papantoniou D (1993a) PTV in 3-D flows; Part II: Particle Tracking. *Experiments in Fluids* 15:279–294

Malik NA, Dracos T, and Papantoniou DA (1993b) Particle tracking velocimetry in three-dimensional flows. *Experiments in Fluids* 15:279–294

Murata S and Yasuda N (2000) Potential of digital holography in particle measurement. *Optics and Laser Technology* 32:567–574

Palero V, Arroyo MP, and Soria J (2007) Digital holography for micro-droplet diagnostics. *Experiments in Fluids* 43:185–195

Pan G and Meng H (2003) Digital holography of particle fields: reconstruction by use of complex amplitude. *Applied Optics* 42:827–833

Sato YK, Kasagi N, and Takamura N (1994) Application of the three-dimensional particle tracking velocimeter to a turbulent air ßow. in *Proceedings of third Asian Symposium on Visualization*. pages 705 – 709

Shi S, Ding J, Atkinson C, Soria J, and New TH (2018) A detailed comparison of single-camera light-field PIV and tomographic PIV. *Experiments in Fluids* 59:1690

Shi S, Ding J, New TH, and Soria J (2017) Light-field camera-based 3D volumetric particle image velocimetry with dense ray tracing reconstruction technique. *Experiments in Fluids* 58:78

von Ellenrieder K and Soria J (2003) Experimental measurements of particle depth of field in digital holography. in *International Workshop on Holographic metrology in Fluid Mechanics*